Eur. Phys. J. A **24**, 199–204 (2005)
DOI 10.1140/epja/i2004-10136-3

THE EUROPEAN PHYSICAL JOURNAL A

High-spin states and band structures in the doubly odd ^{136}La nucleus

S.J. Zhu[1,a], S.D. Xiao[1], X.L. Che[1], Y.N. U[1], M.L. Li[1], Y.J. Chen[1], L.H. Zhu[2], G.S. Li[2], S.X. Wen[2], and X.G. Wu[2]

[1] Department of Physics, Tsinghua University, Beijing 100084, PRC
[2] China Institute of Atomic Energy, Beijing, 102413, PRC

Received: 25 November 2004 / Revised version: 9 January 2005 /
Published online: 11 March 2005 –
Communicated by D. Schwalm

Abstract. High-spin states of ^{136}La have been investigated with the reaction ^{130}Te(^{11}B, 5n) at a beam energy of 60 MeV. The level scheme with three collective bands has been updated with spin up to 20 $\hbar$. The observed $\pi h_{11/2} \otimes \nu h_{11/2}$ band shows γ-instability with increasing spin according to the TRS calculations. The band crossing and the signature splitting and inversion have been discussed. Other two collective bands based on $12^-$and 16^+ levels were proposed as oblate deformation with $\gamma \sim -60°$. They most probably originate from four- and six-quasiparticle configurations, that is, $\pi h_{11/2} \otimes \nu g_{7/2} h^2_{11/2}$ and $\pi g_{7/2} \otimes \nu g^2_{7/2} d_{5/2} h^2_{11/2}$ respectively.

PACS. 23.20.Lv γ transitions and level energies – 21.10.Re Collective levels – 21.60.Ev Collective models

1 Introduction

The doubly odd ^{136}La nucleus lies in the $A = 135$ transitional region with the proton and neutron numbers approaching the closed shells at $Z = 50$ and $N = 82$. It was expected that the ground state of ^{136}La has small quadrupole deformation parameter β and soft γ-deformation. At the high-spin states, the level structures should exhibit complex behaviors. For the nuclei in this region, the neutron Fermi surface lies near the top of the $h_{11/2}$ subshell, while the proton Fermi surface lies in the lower part of the same subshell. Following the increasing rotational frequency, the rotational alignment of a pair of $h_{11/2}$ protons from the lower $h_{11/2}$ midshell drives the nucleus to a near prolate ($\gamma \sim 0°$) shape, while the rotational alignment of a pair of $h_{11/2}$ neutrons from the upper $h_{11/2}$ midshell drives the nucleus to a near oblate ($\gamma \sim -60°$) shape [1] (in the Lund convention [2]). Therefore, the different quasiparticle configurations can drive a nucleus to form different shapes. In some nuclei, shape coexistence can be observed [3]. In the previous reports, one of the important structures in this region is the observation of the oblate bands, for examples, in ^{134}La [4], ^{135}La [5], ^{137}Ce [6] and ^{138}Ce [7]. On the other hand, the chiral doublet bands, for example, reported in ^{132}Cs [8] and ^{134}La [4] and the systematical signature splitting and inversion [9] are also remarkable topics in the doubly odd nuclei.

In order to obtain the systematic information on nuclear structures in this region, it is necessary to explore continuously the neighboring heavier doubly odd nuclei. In this paper, we report on experimental investigation of high-spin states and collective-band structures in ^{136}La. Prior to this work, some lower spin levels in ^{136}La were reported by the (p, 3n) reaction [10], and some high-spin structures have been briefly presented in a recent report [11].

2 Experiment and results

The ^{136}La nucleus was produced using the ^{130}Te (^{11}B, 5n) fusion-evaporation reaction at a beam energy of 60 MeV. An isotopically enriched ^{130}Te target of thickness 1.6 mg/cm^2 was bombarded by the beam of ^{11}B ions accelerated by the HI-13 tandem accelerator at the China Institute of Atomic Energy (CIAE). An array of fourteen Compton-suppressed Ge detectors was employed to measure the in-beam γ-rays. The energy resolutions of the Ge detectors are between 1.8 and 2.2 keV at 1.333 MeV γ-ray energy. The relative excitation function measurements, carried out using beam energies of 50, 55, 60, 65 and 70 MeV, were used to identify the γ-rays from the (^{11}B, 4n), the (^{11}B, 5n) and the (^{11}B, 6n) reactions, respectively. Approximately 50×10^6 background-subtracted coincidence events were collected, from which a γ-γ coincidence matrix was built. The γ-ray energies and relative

[a] e-mail: zhushj@mail.tsinghua.edu.cn

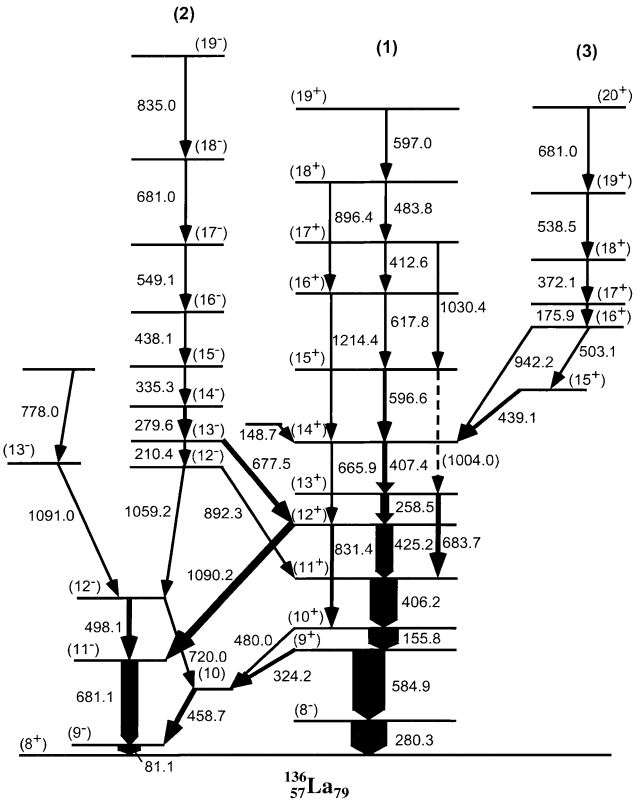

Fig. 1. Level scheme of ^{136}La.

efficiencies were calibrated with a ^{152}Eu source. In order to determine the multipolarities of γ-ray transitions, the five detectors near 90° with respect to the beam axis were sorted against the other nine detectors at 45° (three), 55° (one), 125° (one) and 135° (four), to produce a two-dimensional angular-correlation matrix from which it was possible to extract the average correlation of oriented state (DCO) intensity ratios. The γ-γ coincidence data were analyzed with the Radware software package [12].

The level scheme of ^{136}La constructed in the present work is shown in fig. 1. It was deduced from the γ-γ coincidence relationships, the relative transition intensities and the DCO ratio analysis. The collective bands are labelled on the top of the scheme. The results of this analysis are given in table 1, including the γ-transition energies, the relative intensities of the transitions, the DCO ratios, the γ-transition multipolarities, and the assignments of spin and parity (I^π) values. The γ-transition intensities have been normalized to that of the 280.3 keV ($(8^-) \rightarrow (8^+)$) γ-ray. As the statistics of the DCO data is poorer than that in the total γ-γ coincidence matrix, the DCO values of some week γ-peaks could not been determined. In general, the DCO ratios are larger than 1.0 for $\Delta I = 1$ transitions and less than 0.9 for $\Delta I = 2$ transitions. Some of the sample coincidence γ-ray spectra are shown in figs. 2 and 3. In each spectrum, one can see corresponding coincidence γ-peaks in bands (1), (2) and (3) as well as those between the low-spin states.

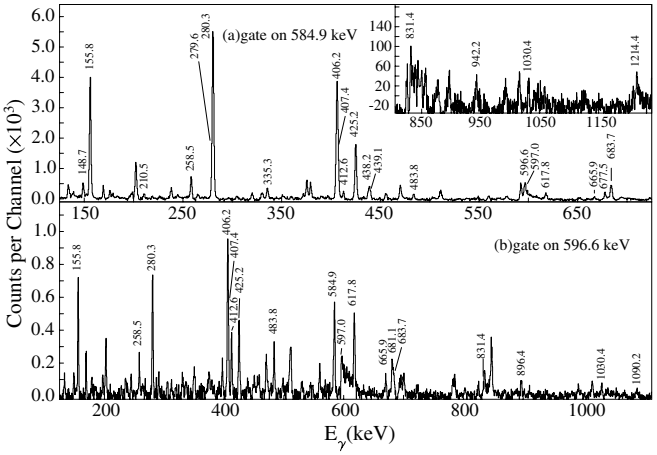

Fig. 2. Coincidence spectra by gating on (a) 584.9 keV and (b) 596.6 keV γ-transitions of band (1).

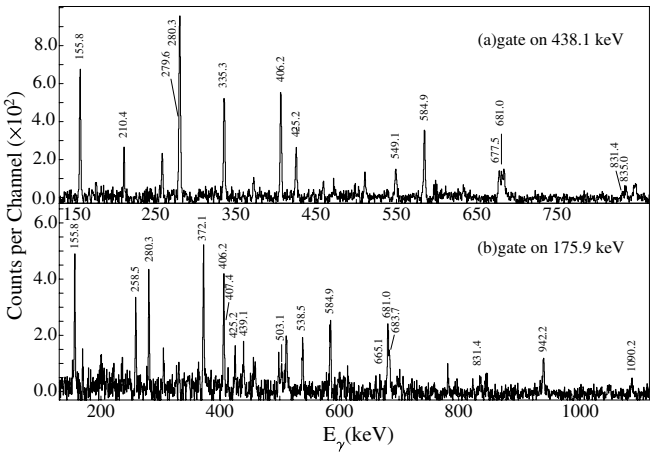

Fig. 3. Coincidence spectra by gating on (a) 438.1 keV γ-transitions in band (2) and (b) the 175.9 keV one in band (3).

In the previous report, the I^π of the ground state in ^{136}La was assigned as 1^+ [10]. An isomer with 115 ms half-life has been observed and the I^π for this isomer was tentatively assigned as 8^- or 7^- [10]. In ref. [11] the lowest level of the level scheme was assumed to be based on this isomer level with spin and parity 8^+. We tentatively assigned the I^π of the lowest level in fig. 1 as 8^+ also. The I^π's of the other levels are tentatively assigned based on the previous data [10,11], the DCO ratios and the systematic comparison with the neighboring La isotopes. At the low spins, we confirmed that the 324.2 keV transition lies above the 458.7 keV one as reported in ref. [10], but not in ref. [11]. This assignment was further supported by observing the 480.0 and 720.0 keV linking transitions. A new transition of 1092.2 keV from the 12^+ level in band (1) to the 11^- level has also been identified. There are three band structures as labelled in fig. 1. Comparing our result with those in the previous reports [10,11], band (1) has been obviously extended and updated . Some levels and transitions of band (1) reported in ref. [11] were not confirmed in the present work. We reconstructed the levels from 13^+ to 19^+ states. As a few linking $\Delta I = 2$ transitions were

Table 1. Energies, intensities and DCO ratio data of the transitions in ^{136}La.

E_γ [a] (keV)	Intensities (%)	DCO ratio	Assignment	Multipolarity	Band
81.1			$(9^-) \rightarrow (8^-)$		
148.7	1.2(2)	1.56(20)	$\rightarrow (14^+)$		
155.8	86.2(8)	1.19(6)	$(10^+) \rightarrow (9^+)$	$M1/E2$	(1)
175.9	4.5(3)	1.14(10)	$(17^+) \rightarrow (16^+)$	$M1/E2$	(3)
210.4	0.6(1)	1.47(30)	$(13^-) \rightarrow (12^-)$	$M1/E2$	(2)
258.5	17.1(7)	1.27(9)	$(13^+) \rightarrow (12^+)$	$M1/E2$	(1)
279.6	14.7(6)	1.13(8)	$(14^-) \rightarrow (13^-)$	$M1/E2$	(2)
280.3	100	1.09(4)	$(8^-) \rightarrow (8^+)$	$(E1)$	
324.2	8.7(5)		$(9^+) \rightarrow (10)$		(1) $\rightarrow$
335.3	5.4(3)	1.10(9)	$(15^-) \rightarrow (14^-)$	$M1/E2$	(2)
372.1	3.0(2)	1.26(13)	$(18^+) \rightarrow (17^+)$	$M1/E2$	(3)
406.2	70.4(8)	1.09(6)	$(11^+) \rightarrow (10^+)$	$M1/E2$	(1)
407.4	16.2(7)	1.09(8)	$(14^+) \rightarrow (13^+)$	$M1/E2$	(1)
412.6	2.4(2)	1.06(12)	$(17^+) \rightarrow (16^+)$	$M1/E2$	(1)
425.2	46.5(7)	1.22(6)	$(12^+) \rightarrow (11^+)$	$M1/E2$	(1)
438.1	3.1(2)	1.13(9)	$(16^-) \rightarrow (15^-)$	$M1/E2$	(2)
439.1	4.8(3)	1.28(10)	$(15^+) \rightarrow (14^+)$	$(M1/E2)$	$\rightarrow$ (1)
458.7	14.3(6)	1.14(8)	$(10) \rightarrow (9^-)$		
480.0	0.9(2)		$(10^+) \rightarrow (10)$		(1) $\rightarrow$
483.8	2.1(3)	1.23(20)	$(18^+) \rightarrow (17^+)$	$M1/E2$	(1)
498.1	11.2(5)	1.42(9)	$(12^-) \rightarrow (11^-)$	$(M1/E2)$	
503.1	2.0(2)		$(16^+) \rightarrow (15^+)$	$(M1/E2)$	(3) $\rightarrow$
538.5	2.1(2)		$(19^+) \rightarrow (18^+)$	$M1/E2$	(3)
549.1	1.4(2)	1.18(19)	$(17^-) \rightarrow (16^-)$	$M1/E2$	(2)
584.9	91.3(9)	1.19(5)	$(9^+) \rightarrow (8^-)$	$(E1)$	
596.6	4.5(2)	1.12(9)	$(15^+) \rightarrow (14^+)$	$M1/E2$	(1)
597.0	1.5(2)		$(19^+) \rightarrow (18^+)$	$(M1/E2)$	(1)
617.8	3.1(3)	1.09(11)	$(16^+) \rightarrow (15^+)$	$M1/E2$	(1)
665.9	1.1(2)		$(14^+) \rightarrow (12^+)$	$E2$	(1)
677.5	17.3(7)	1.28(8)	$(13^-) \rightarrow (12^+)$	$(E1)$	(2) $\rightarrow$ (1)
681.0	1.0(2)		$(20^+) \rightarrow (19^+)$	$M1/E2$	(3)
681.1	51.2(8)	0.78(5)	$(11^-) \rightarrow (9^-)$	$(E2)$	
681.6	1.1(2)		$(18^-) \rightarrow (17^-)$	$M1/E2$	(2)
683.7	19.4(6)	0.79(6)	$(13^+) \rightarrow (11^+)$	$E2$	(1)
720.0	2.8(3)		$(12^+) \rightarrow (10)$		
778.0	< 0.5		$\rightarrow (13^-)$		
831.4	10.1(4)	0.81(8)	$(12^+) \rightarrow (10^+)$	$E2$	(1)
835.0	1.0(2)		$(19^-) \rightarrow (18^-)$	$M1/E2$	(2)
892.3	2.5(2)		$(12^-) \rightarrow (11^+)$	$(E1)$	(2) $\rightarrow$ (1)
896.4	0.6(2)		$(18^+) \rightarrow (16^+)$	$E2$	(1)
942.2	3.0(3)	0.88(11)	$(16^+) \rightarrow (14^+)$	$(E2)$	(3) $\rightarrow$ (1)
(1004.0)			$(15^+) \rightarrow (13^+)$	$(E2)$	(1)
1030.4	0.9(3)		$(17^+) \rightarrow (15^+)$	$E2$	(1)
1059.2	4.4(3)		$(12^-) \rightarrow (12^-)$	$(M1/E2)$	(2) $\rightarrow$
1090.2	35.7(6)	1.14(7)	$(12^+) \rightarrow (11^-)$	$(E1)$	(1) $\rightarrow$
1091.0	7.5(5)		$(13^-) \rightarrow (12^-)$	$(M1/E2)$	
1214.1	1.4(2)	0.82(15)	$(16^+) \rightarrow (14^+)$	$E2$	(1)

[a] The errors for all γ-energies are in less than 0.5 keV.

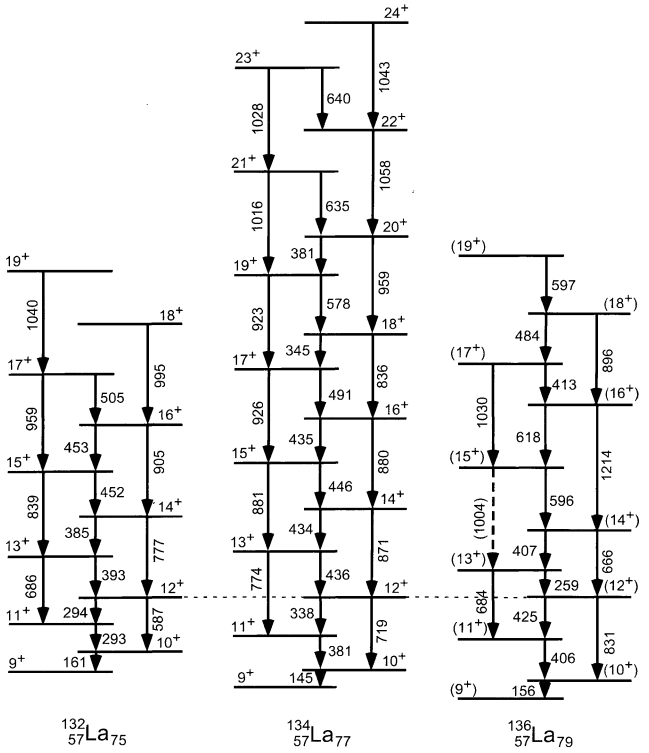

Fig. 4. The level systematics of the $\pi h_{11/2} \otimes \nu h_{11/2}$ bands in ^{132,134,136}La. The states with $I = 12\hbar$ are taken as reference for comparison. Energies are given in keV.

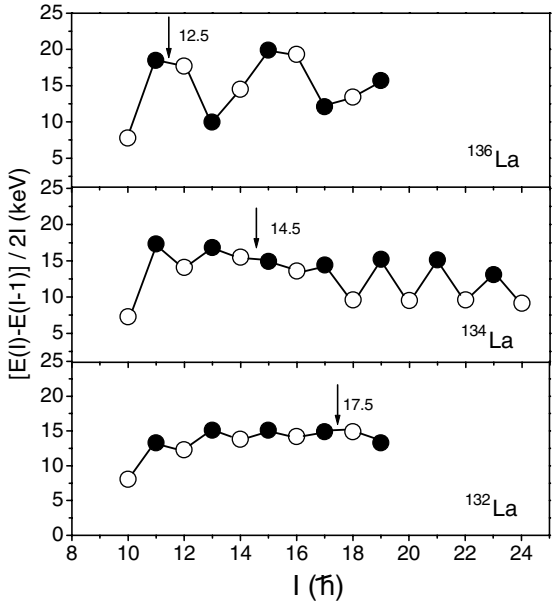

Fig. 5. $[E(I) - E(I-1)]/2I$ *versus* I for the $\pi h_{11/2} \otimes \nu h_{11/2}$ bands in ^{132,134,136}La.

also identified, it may give further evidence for the level assignments of band (1). Band (2) was observed in ref. [11]. We confirmed this band and added a new level along with a new transition of 835.0 keV above it. We extended band (3) by two levels and two transitions of 538.5 and 681.0 keV, and so band (3) was firmly established. The linking transitions between bands (1) and (3) have been newly arranged also.

3 Discussion

3.1 Band (1)

In the previous report, yrast band (1) was assigned as even-parity band based on the 8^+ level [11]. However, through a systematic comparison with the neighboring doubly odd La isotopes, we tentatively assigned the I^π of the band head level as 9^+. Thus, the spin value for each level in this band differs by 1 $\hbar$ between the result in this work and that in ref. [11]. This band has been considered as the $\pi h_{11/2} \otimes \nu h_{11/2}$ configuration [11]. Figure 4 shows the systematic levels of the $\pi h_{11/2} \otimes \nu h_{11/2}$ bands observed in ^{132}La [13], ^{134}La [4] and ^{136}La in this work. According to the systematics of $\pi h_{11/2} \otimes \nu h_{11/2}$ bands in the $A = 130$ region by Liu *et al.* [9], the spin value 9 $\hbar$ of the band head of band (1) in ^{136}La should be a reasonable assignment.

The signature inversion in the rotational spectra of the $\pi h_{11/2} \otimes \nu h_{11/2}$ bands in doubly odd nuclei of the $A = 130$ light rare-earth region has been paid attention to and systematically studied by many authors, for example, in ref. [9]. Figure 5 shows the plots of $[E(I) - E(I-1)]/2I$ *versus* spin I for the $\pi h_{11/2} \otimes \nu h_{11/2}$ bands of ^{132}La [13], ^{134}La [4] and ^{136}La in this work. It indicates that at the low-spin states, the $\pi h_{11/2} \otimes \nu h_{11/2}$ band in ^{136}La indeed shows the signature inversion. The spin value for the inversion point $I_{\rm inv}$ is reduced with increasing neutron number: 17.5 $\hbar$ for ^{132}La, 14.5 $\hbar$ for ^{134}La and 12.5 $\hbar$ for ^{136}La. It is notable that when $I \geq I_{\rm inv}$, no signature inversion occurs in the lighter doubly odd La isotopes ($N \leq 75$) and signature inversion still occurs in ^{134}La ($N = 77$), while the signature splitting shows an irregularity in ^{136}La ($N = 79$). This phenomenon needs more theoretical work to be explained.

Examining band (1) in ^{136}La, at the lower spins, the level spacings show an irregularity. However, above the 12^+ level, they become more regular. At the spin $I = 16$–$18\hbar$, a band crossing (backbending) occurs at $\hbar\omega \approx 0.45$ MeV. Since ^{136}La lies in a transition region with neutron number approaching the closed shell at $N = 82$, a soft potential energy surface and configuration-dependent deformation can be expected. In order to understand the properties of the deformation and band crossing in the $\pi h_{11/2} \otimes \nu h_{11/2}$ band in ^{136}La, we have carried out cranked-shell model (CSM) calculations described in detail by Bengtsson and Frauendorf [14–16]. The calculations in this work are involved with the total Routhian surfaces (TRS) and Routhians. The calculated results of the CSM indicate that with increasing spin, the value of the quadrupole deformation parameter β_2 varies between 0.10 and 0.14, and the γ-value varies between $-30°$ and $20°$ for the $\pi h_{11/2} \otimes \nu h_{11/2}$ band. Figure 6 shows two plots of the TRS of the $\pi h_{11/2} \otimes \nu h_{11/2}$ band in ^{136}La, where the minima can be found as $\beta_2 = 0.139$,

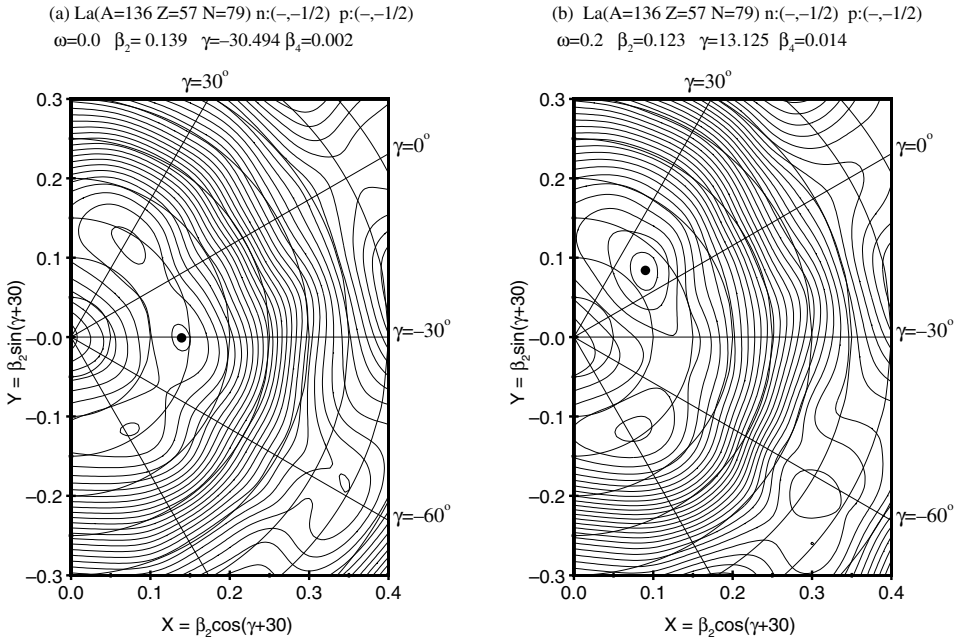

Fig. 6. Plots of the total Routhian surface (TRS) calculated (a) at $\hbar\omega = 0.0$ MeV and (b) at $\hbar\omega = 0.2$ MeV for ^{136}La.

$\gamma = -30°$ at $\omega = 0$ MeV/$\hbar$ and $\beta_2 = 0.123$, $\gamma = 13°$ at $\omega = 0.2$ MeV/$\hbar$, respectively. The calculated results indeed show γ-instability with increasing spin. The calculated quasiparticle energies (Routhians) for ^{136}La are presented in fig. 7a for protons and in fig. 7b for neutrons, respectively. The calculations predict that a band crossing caused by the alignment of two $h_{11/2}$ neutrons occurs at $\hbar\omega \approx 0.44$ MeV, which is close to the experimental value of $\hbar\omega \approx 0.45$ MeV, whereas the band crossing related to the alignment of two protons shows an irregularity. Hence, we believe that the $h_{11/2}$ neutron orbital is responsible for the backbending in the $\pi h_{11/2} \otimes \nu h_{11/2}$ band in ^{136}La. This explanation is in accord with the systematics as the same interpretation for the backbending was given in the neighboring doubly odd ^{134}La nucleus [4].

3.2 Bands (2) and (3)

Bands (2) and (3), built on the 12^- and 13^+ levels respectively, have similar structural character. Based on a systematic comparison with the neighboring nuclei in this region, for example, ^{137}Ce [6], ^{138}Ce [7], ^{134}La [4] and ^{135}La [5], we believe that these two bands in ^{136}La should belong to collective oblate bands built on multi-quasiparticle configurations with $\gamma = -60°$. The observed oblate bands exhibit some distinct features: a) much stronger $\Delta I = 1$ transitions relative to the $\Delta I = 2$ ones inside the band, b) dipole transitions increasing regularly in energy, that is, without signature splitting, and c) different moment of inertia from those of prolate bands. Bands (2) and (3) in ^{136}La are just to exhibit the above features. Plots of the moment of inertia $J^{(1)}$ of bands (2) and (3) in ^{136}La along with the observed oblate bands in ^{134}La [4] and ^{137}Ce [6] against the rotational frequency $\hbar\omega$ are shown in fig. 8. The $J^{(1)}$'s of bands (2) and (3) in ^{136}La show a behavior similar to that of the oblate bands in the neighboring nuclei and they decrease with increasing $\hbar\omega$.

In ref. [11], band (2) of ^{136}La has been tentatively assigned a $\pi[413]_{5/2}h^2_{11/2}\otimes\nu h_{11/2}$ configuration. We disagree with such assignment. If this assignment were right, a pair of $h_{11/2}$ protons should drive the nucleus to form a prolate shape instead of the oblate one. From the systematical comparison, we think that the possible configuration for the oblate band (2) is $\pi h_{11/2} \otimes \nu g_{7/2}h^2_{11/2}$, which is same as that in the oblate band (5) of ^{134}La [4]. Thus, a pair of $h_{11/2}$ neutrons should drive the nucleus to form the oblate shape. As the excitation energy of the band head in the even-parity band (3) is higher than that in band (2), band (3) may originate from a six-quasiparticle configuration, for example, $\pi g_{7/2} \otimes \nu g^2_{7/2}d_{5/2}h^2_{11/2}$. In the previous works, the shape-driving effects of proton and neutron in this region have been discussed in terms of the CSM calculations [1,17]. They show that the alignment of a pair of $h_{11/2}$ protons favors a prolate shape ($\gamma \sim 0°$) and the alignment of a pair of $h_{11/2}$ neutrons favors an oblate shape ($\gamma \sim -60°$). For the oblate shape ($\gamma \sim -60°$), high-Ω $h_{11/2}$ protons and low-Ω $h_{11/2}$ neutrons are near the Fermi surface. Such high-Ω $h_{11/2}$ protons enhance the $B(M1)$ transition rates within the band. The largest enhancement of the $B(M1)$ transition rates will occur for a coupled $\pi h_{11/2}[505]_{11/2}$ orbital at $\gamma \sim -60°$ [1]. On the other hand, the signature splitting of the $h_{11/2}$ proton orbital strongly depends on the γ value. As γ approaches $-60°$ (oblate shape), the splitting of the proton orbital approaches zero, so no signature splitting occurs in the oblate bands.

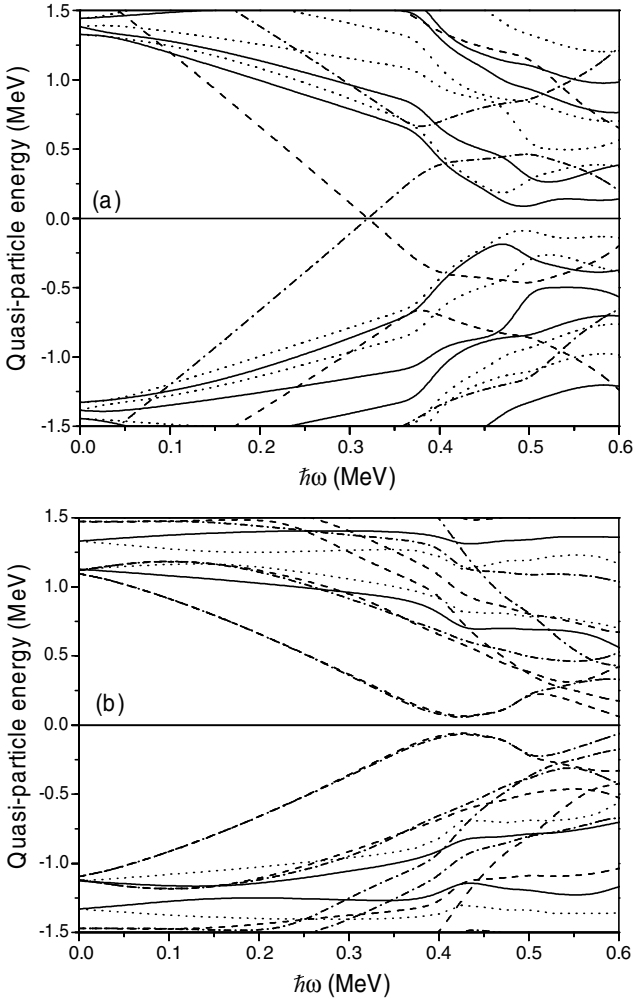

Fig. 7. Plots of the calculated Routhians for quasiprotons and quasineutrons against the rotational frequency $\hbar\omega$. The parity and signature (π, α) of the levels are: $(+1/2, +1/2)$ solid lines; $(+1/2, -1/2)$ dotted lines; $(-1/2, +1/2)$ dot-dashed lines; $(-1/2, -1/2)$ dashed lines.

4 Conclusions

High-spin states in the doubly odd ^{136}La nucleus have been studied. The previous level scheme has been updated. Many new levels and transitions were identified. The signature splitting and inversion in the $\pi h_{11/2} \otimes \nu h_{11/2}$ band have been discussed. The CSM calculations indicate that the $\pi h_{11/2} \otimes \nu h_{11/2}$ band shows γ-instability with increasing spin and the band crossing observed in $\pi h_{11/2} \otimes \nu h_{11/2}$ band is caused by a pair of $h_{11/2}$ neutrons alignment. Two oblate bands with $\gamma \sim -60°$ have been observed, which may originate from the $\pi h_{11/2} \otimes \nu g_{7/2} h^2_{11/2}$ and $\pi g_{7/2} \otimes \nu g^2_{7/2} d_{5/2} h^2_{11/2}$ configurations, respectively. No chiral doublet band structure was found in this doubly odd nucleus.

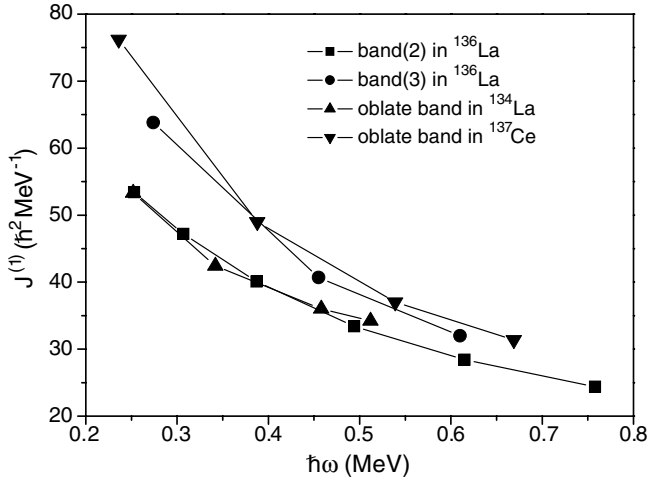

Fig. 8. Plots of the moment of inertia ($J^{(1)}$) *versus* the rotational frequency $\hbar\omega$ for bands (2) and (3) in ^{136}La as well as for the oblate bands in ^{134}La and ^{137}Ce.

The work at Tsinghua University was supported by the National Natural Science Foundation of China under Grant No. 10375032, the Major State Basic Research Development Program under Contract No. G2000077405, the Special Program of Higher Education Science Foundation under Grant No. 20030003090. The authors wish to thank the staff of the in-beam γ-ray group and the tandem accelerator group at CIAE for their help and hospitality during the experiment and for providing the heavy-ion beam and the target. The authors are also thankful to Xu Fu-Rong and Wu Zhe-Ying at Peking University for helping with the CSM calculations and very enlightening discussions.

References

1. E.S. Paul *et al.*, Phys. Rev. Lett. **58**, 984 (1987).
2. G. Andersson *et al.*, Nucl. Phys. A **268**, 205 (1976).
3. E.S. Paul *et al.*, Phys. Rev. C **40**, 1255 (1989).
4. R.A. Bark *et al.*, Nucl. Phys. A **691**, 577 (2001).
5. P. Luo *et al.*, High Energy Phys. Nucl. Phys. **28**, 495 (2004) (in Chinese).
6. S.J. Zhu *et al.*, Phys. Rev. C **62**, 044310 (2000).
7. S.J. Zhu *et al.*, Chin. Phys. Lett. **16**, 635 (1999).
8. G. Rainovski *et al.*, J. Phys. G **29**, 2763 (2003).
9. Y. Liu *et al.*, Phys. Rev. C **54**, 719 (1996).
10. T. Morek *et al.*, Nucl. Phys. A **433**, 159 (1985).
11. E.W. Cybulska *et al.*, Acta Phys. Pol. B **32**, 929 (2001).
12. D.C. Radford, Nucl. Instrum. Methods A **361**, 297 (1995).
13. V. Kumar *et al.*, Eur. Phys. J. A **17**, 153 (2003).
14. R. Bengtsson *et al.*, Nucl. Phys. A **237**, 139 (1972).
15. S. Frauendorf *et al.*, Phys. Lett. B **100**, 219 (1981).
16. S. Frauendorf *et al.*, Phys. Lett. B **125**, 219 (1983).
17. K. Hauschild *et al.*, Phys. Rev. C **54**, 613 (1996).